# Portable and label-free quantitative Loop-mediated Isothermal Amplification (qLAMP) for reliable COVID-19 diagnostics in 3 minutes: An Arduino-based detection system assisted by a pH microelectrode

Mario Moisés Alvarez[1,2,*], Sergio Bravo-González[1,2], Everardo González-González[1,2], Grissel Trujillo-de Santiago[1,3,*],

1) *Centro de Biotecnología-FEMSA, Tecnologico de Monterrey, Monterrey 64849, NL, México*
2) *Departamento de Bioingeniería, Escuela de Ingeniería y Ciencias, Tecnologico de Monterrey, Monterrey 64849, NL, México*
3) *Departamento de Ingeniería Mecatrónica y Eléctrica, Escuela de Ingeniería y Ciencias, Tecnologico de Monterrey, Monterrey 64849, NL, México*

(*) corresponding authors: *grissel@tec.mx; mario.alvarez@tec.mx*

## Abstract

Loop-mediated isothermal amplification (LAMP) has been recently studied as an alternative method for cost-effective diagnostics in the context of the current COVID-19 pandemic. Recent reports document that LAMP-based diagnostic methods have a comparable sensitivity and specificity to that of RT-qPCR. We report the use of a portable Arduino-based LAMP-based amplification system assisted by pH microelectrodes for the

accurate and reliable diagnosis of SARS-CoV-2 during the first 3 minutes of the amplification reaction. We show that this simple system enables a straightforward discrimination between samples containing or not containing artificial SARS-CoV-2 genetic material in the range of 10 to 10,000 copies per 50 µL of reaction mix. We also spiked saliva samples with SARS-CoV-2 synthetic material and corroborated that the LAMP reaction can be successfully monitored in real time using microelectrodes in saliva samples as well. These results may have profound implications for the design of real-time and portable quantitative systems for the reliable detection of viral pathogens including SARS-CoV-2.

Keywords: SARS-CoV-2, COVID-19, qLAMP, amplification, diagnostics, electrodes.

To be submitted to

*Biosensors and Bioelectronics*

# Introduction

At present, nearly 150 million people have been diagnosed with COVID-19 (+) worldwide, and the disease has killed more than 3 million people [1], making it the most lethal infectious disease in a century. COVID-19 has laid bare the severe limitations in our capacities to respond to epidemic emergencies and has made clear that we must expand and strengthen the portfolio of available tools for effective diagnostics of infectious diseases [2] both now and in the future.

The retro-transcriptase quantitative polymerase chain reaction (RT-qPCR) is currently the gold standard methodology for COVID-19 detection [2–5]. Despite its unquestionable accuracy and robustness, qPCR-based methods have some serious limitations (e.g., lack of

47 portability, dependence on centralized facilities, need for technical expertise to conduct RT-
48 qPCR testing, and high infrastructural and operative costs) that prevent the provision of
49 cost-effective and massive diagnostics during this time of COVID-19 [2,6,7].

50 One potential alternative to RT-qPCR could be Loop-mediated Isothermal Amplification
51 (LAMP), which has been extensively studied in recent reports as a cost-effective diagnostic
52 system in the context of the current COVID-19 pandemic [8–16]. Overall, these reports
53 have documented that LAMP-based methods have comparable sensitivity and specificity to
54 that of RT-qPCR. More importantly, LAMP methods provide attractive advantages over
55 RT-qPCR methods in terms of lower capital and operating costs. LAMP is an isothermal
56 method, so it frees the user from the need for a costly thermal cycler. In addition, LAMP
57 methods that exhibit excellent sensibility and acceptable specificity have been described for
58 the extraction-free analysis of nasopharyngeal and even saliva samples [15,17,18]. The
59 release from the need for an extraction stage further reduces the cost of LAMP
60 methodology.

61 Most LAMP-based methods rely on a discrimination between positive and negative
62 samples due to a change in the pH associated with an acidification of the reaction mix due
63 to the liberation of hydrogen ions ($H_3O^+$) inherent in the amplification [15,17,19]. In a
64 weakly buffered reaction medium, the change in pH may translate into a change in color if
65 a pH indicator is added to the reaction mix. A frequent embodiment of colorimetric LAMP
66 uses phenol red as the pH indicator [17,19–21] and a weak buffer that contains mainly Tris-
67 HCl, $(NH4)_2SO_4$ (ammonium sulfate), and KCl (potassium chloride).

68 However, colorimetric LAMP methods also have some limitations. One is that the adequate
69 performance of colorimetric LAMP mediated by phenol red depends on the initial pH of the

sample. This is particularly relevant in extraction-free applications, since acidic samples may prematurely shift the color of the reaction mix, even in non-infected saliva samples, thereby possibly rendering false positives. LAMP-based methods also use from four to six primer sets, and the design of LAMP primer sets is nontrivial as the primers may interact among themselves during amplification. This can promote non-specific amplifications that may also result in false positives[22,23].

In the present study, we demonstrate the straightforward use of microelectrodes to monitor, in real time, the evolution of the amplification of SARS-CoV-2 genetic material. This simple implementation renders a quantitative and label-free embodiment of the LAMP reaction (LF-LAMP) for amplification of any genetic sequence. Label free quantitative LAMP (LF-qLAMP) allows the continuous and online monitoring of the change in the electric potential of the reaction mix due to the release of hydrogen ions during amplification. We show that the progressions of the signal from truly positive samples (samples containing genetic material from SARS-CoV-2) and negative samples clearly differ in LF-qLAMP. Therefore, this method provides a straightforward way to distinguish pH shifts that are truly due to specific amplifications and are not false positives.

In this time of COVID-19, we also illustrate LF-qLAMP for the diagnostics of COVID-19 from saliva samples spiked with SARS-CoV-2 nucleic acids. Overall, we demonstrate the utility of extraction-free LF-LAMP for COVID-19 from samples containing artificial SARS-CoV-2 genetic material and from saliva samples containing artificial SARS-CoV-2 genetic material.

## Materials and methods

*Equipment specifications:*

We fabricated a simple and portable prototype for the isothermal incubation of samples and online monitoring of the LAMP amplification process using a commercial and low-cost pH sensor (Gaohau pH 0–14; available at Amazon.com; USA), a commercial pH electrode (inLab nano; Mettler Toledo, Switzerland), and an Arduino UNO® microprocessor (Arduino, Italy).

This *ad hoc* heating system was assembled with components acquired over the internet (amazon.com) and consisted of a 12V eliminator, a 10 mL vessel with a silicon lead, a heating mat (electric resistance), and an Arduino UNO–based proportional integral derivative (PID) temperature controller (fully described in the supplementary material). The Arduino-based PID controller is depicted in Figure 2A and Figure S1. The code used in our heating/amplification experiments has been made available as supplementary material (Supplementary file 1).

The evolution of the amplification process was followed using commercially available pH electrodes (inLab nano, from Mettler Toledo, Switzerland; and Lab Sen 241-3, from Aprea Instruments, available at Amazon.com). These electrodes were interfaced through an Arduino UNO microprocessor using a pH sensor module (Gaohou pH 0-14 detect sensor module, available at Amazon.com). The InLab microelectrode, with a tip diameter of 1.3 mm, can be easily placed inside a conventional 200 µL Eppendorf tube and enables the use of small reaction volumes (25–50 µL of reaction mix and sample). Alternatively, we have run online experiments using a lower cost electrode from Apera Instruments (~150 USD)

with a tip diameter of 3 mm, which can also be used with similar measuring performance (supplementary material; Figure S1) if a larger reaction volume is used (~50 µL).

In our experiments, the insertion of the electrode within the reaction mix impedes closure of the Eppendorf tube during incubation. To avoid evaporation during heating, two drops of mineral oil were dispensed into each Eppendorf tube before electrode placement to allow the development of a thin lid layer of mineral oil at the liquid surface of the reaction mix. The Arduino code used in the experiments reported here are available as supplemental material (Supplemental file 1).

*Experiments with synthetic genetic material:* We ran several series of experiments where samples containing different quantities of SARS-CoV-2 synthetic genetic material were analyzed using LF-qLAMP. These amplification experiments were conducted using the homemade system previously described for isothermal heating of the samples at 62.5 +/- 1.5 °C and for online monitoring of the progression of the electric potential in the reaction mix during amplification.

Samples were prepared by adding 4 µL of a solution containing the DNA template to 250 µL Eppendorf tubes containing 25 µL WarmStart® Colorimetric LAMP 2× Master Mix (DNA & RNA) from New England Biolabs (MA, USA), 18 µL nucleasease-free water from New England Biolabs (MA, USA), and 2 µL primer solution. Samples were prepared by adding different quantities of positive DNA templates (i.e., 0, 10, 100, 1,000, and 10,000 copies of the gene N from SARS-CoV-2; Integrated DNA Technologies, IA, USA). Negative amplification controls were prepared using the reaction mix, as previously described, but without primer addition.

*Preparation of saliva samples spiked with RNA extracts:* A set of 5 saliva samples obtained from healthy volunteers was spiked with different quantities of SARS-CoV-2 synthetic genetic material. Saliva samples were also collected from a COVID-19(+) patient after obtaining written consent and in full compliance with the principles stated in the Helsinki Declaration. Every precaution has been taken to protect the privacy of sample donors and the confidentiality of their personal information. Our experimental protocols for saliva collection and saliva use in amplification was approved, as part of a wider study to collect and test saliva samples from human volunteers, by the Alfa Medical Research Committee in the resolution AMCCI-TECCOVID-001 on May 20th, 2020 (Alfa Medical Center, Research Committee; Monterrey, NL, México). Saliva samples were inactivated by heat treatment at 62.5 °C for 35 minutes prior to amplification.

*Amplification mix:* We used WarmStart® Colorimetric LAMP 2× Master Mix (DNA & RNA) from New England Biolabs (MA, USA), and followed the recommended protocol: 25 µL Readymix, 1.6 µM FIP primer, 1.6 µM BIP primer, 0.2 µM F3 primer, 0.2 µM B3 primer, 0.4 µM LF primer, 0.4 µM LB primer, 2 µL DNA template (~ 625 to 2 × $10^5$ DNA copies), and nuclease-free water in a final reaction volume of 50 µL. This commercial mix contains phenol red as a pH indicator to reveal the pH shift occurring during LAMP amplification across the threshold of pH=6.8.

*Primers used:* A sets of six LAMP primers, referred to here as the α-set, was designed in house using the LAMP primer design software Primer Explorer V5 (http://primerexplorer.jp/lampv5e/index.html). These LAMP primers were designed to target a region of the sequence of the SARS-CoV-2 N gene; specifically, they were based

on the analysis of alignments of the SARS-CoV-2 N gene sequences using the Geneious software (Auckland, New Zealand).

RT-qPCR amplification experiments were conducted using one the primer sets recommended by the Centers for Disease Control (CDC) for the standard diagnostics of COVID-19 (i.e., the N1 assay). The sequences of our LAMP primers are presented in Table 1. The sequences of the PCR primers (N1) have been reported elsewhere [24,25].

*Amplification protocols*: For all LAMP experiments, we performed isothermal heating at 62.5 +/- 1.2 °C for 30 to 60 min.

## Results and discussion

### Rationale of the design and operation

Here, we have demonstrated the use a portable Arduino-based LAMP system as a label-free quantitative method (LF-qLAMP) for the reliable and fast identification of samples containing SARS-CoV-2 genetic material. We have introduced a simple and fully portable setup for the detection of viral genetic material using commercially available pH microelectrodes for real-time monitoring of the progression of LAMP reactions. Remarkably, this LAMP-based method is capable of discerning between positive and negative samples during the first three minutes of amplification.

The rationale behind the operation of this strategy is straightforward. In the weakly buffered reaction mix used for LAMP, the release of $H_3O^+$ ions inherent in the amplification process [26] can be measured in real time as a difference in the electric potential[27,28] or a pH change [29,30]. We fabricated a simple and portable prototype to

accomplish two purposes: the isothermal incubation of samples and the online monitoring of the amplification process. To this aim, we used a commercial and low-cost pH sensor, a commercial pH electrode, and an Arduino UNO® microprocessor.

Figure 1 shows the different aspects of this prototype. The isothermal amplification reactions were conducted at 62.5 °C +/- 1.5 °C in 200 µL Eppendorf tubes immersed in a mineral oil bath (Figure 1A) and containing a total reaction mix volume of 50 µL. The tip of a commercial pH microelectrode was immersed into the reaction mix for online monitoring of the progression of the electric potential (in mV) using an Arduino-based system. A simple Arduino code was used to enable the collection and transmission of data to the computer (Supplementary File S1); the difference in the electric potential (ΔP), as evaluated in the reaction solution, was continuously transmitted and recorded at a sampling rate of 1 Hz (i.e., 1 sampling point per second).

The stability of the electric potential readings is affected by temperature fluctuations around the set point. Therefore, adequate temperature control (62.5 +/- 1.5 °C) is highly recommended for conclusive results. In our experiments, executed at home, the temperature within the water bath was controlled at 62.5 °C using the Arduino-based PID controller. For convenience, we have included all the information needed to build this portable and low-cost isothermal PID-incubator for Eppendorf tubes that enables full portability (Figure 1; Figure 2) of the system. Alternatively, the LAMP reaction can be incubated in any commercial thermo block or in a miniPCR® apparatus [31].

**Figure 1**

Figure 2 schematically shows the connections that should be made between the Arduino microcontroller, the low-cost pH sensor, and the rest of the components of the circuit that

205 constitute the PID control system and the online electric potential monitor. Figure S1 (in
206 supplementary material) shows an image of the actual experimental Arduino-based PID
207 controller system.

208 **Figure 2**

209 **Characterization of the performance of the monitoring system**

210 We evaluated the stability of the potential signal at the temperature set point and during
211 temperature ramps. The electric potential is a strong function of the temperature (Figure
212 3A). For instance, the electric potential increased ~90 mV per 10°C in our experiments in
213 the range of 45 to 55 °C. By contrast, at isothermal conditions, the intrinsic variation of the
214 electric potential was very stable; the variations were lower than 0.3% for the range of pH
215 buffers that we assayed.

216 We also analyzed the ability of this simple PID controller to function for extended
217 incubation periods (i.e., 60 minutes) and under different room temperatures (Figure 3B).
218 Overall, we found that this simple incubator system is sufficiently robust to maintain the
219 temperature at the set point (average temperature of 62.5 °C; average standard deviation of
220 0.5 °C) regardless of the room temperature (i.e., in a range between 15 and 25 °C). As we
221 will show, this level of control is sufficient to obtain reliable and reproducible results of
222 determination of the electric potential in solutions with different pH values and during
223 LAMP reactions.

224 In a first set of experiments, we evaluated the robustness and consistency of the
225 characteristics of the electrode readings at different pH values. Figure 3A shows

representative readings associated with the immersion of the microelectrode in buffer solution of different pH values (i.e., pH 6.0, 6.4, 6.8, 7.2, 7.6, and 8.0).

**Figure 3**

The standard deviation associated with the readings within this window of pH values ranges from 1.38 and 6.91 mV (Table S1). For example, the average electric potential measured for a buffer solution at pH 6.8 (which is approximately the threshold value of phenol red) was 2777 mV and exhibited a standard deviation of +/- 1.38 mV.

A buffer solution at pH 8.0 (which is similar to the pH value of the LAMP buffer used) had an electric potential of 2587.58 mV with a standard deviation of +/-6.21 mV. Overall, we observed coefficients of variance lower than 0.3% for all the experiments conducted in the absence of amplification reactions. In all these cases, the electric potential remains essentially stable during incubation periods of 60 minutes. This indicates that the inherent error (i.e., the intrinsic fluctuation associated with the potential signal at the experimental conditions) is in the range of +/- 12.3 mV (i.e., the maximum standard deviations are lower than 7 mV). We also evaluated the stability of the signal reported by the microelectrode when immersed in the buffer of the reaction mix. Our results also suggest that the potential readings obtained using this simple sensing system are robust and steady, with intrinsic coefficients of variance lower than 1%.

**Discrimination between positive and negative samples**

Using the simple Arduino-based system that we have described, we incubated a series of LAMP reactions and monitored the progress of the amplification reaction by measuring the electric potential in the reaction mix in real time. We successfully discriminated between

248 COVID-19(+) and COVID-19(-) samples in a set of synthetic samples and in a set of saliva
249 samples spiked with synthetic SARS-CoV-2 genetic material.

250 We first characterized the baseline corresponding to negative samples, where no primers
251 were added (supplementary material; Figure S2), As expected, the signal associated with
252 these samples was relatively steady (average standard deviations ~10.7; n=3). We then
253 monitored the evolution of the LAMP reactions in the negative samples containing LAMP
254 reaction mix and primers, but no synthetic SARS-CoV-2 genetic material.

255 One of the limitations of colorimetric LAMP-based methods based on the phenol red color
256 shift is that some degree of color change exists in samples containing no template (see also
257 ref [27] ). This has been associated to the occurrence of non-specific amplification induced
258 by the interaction among the LAMP primers [23,32], which often serve as templates for
259 off-target polymerizations. In general, non-specific amplification is believed to be the main
260 reason for false positives in LAMP colorimetric reactions.

261 Figure 4 A shows the typical profile of the progression of the electric potential in negative
262 samples (with primers, reaction mix, but no SARS-CoV-2 template). Four representative
263 replicates are shown. The shape of the progression of the electric potential in the negative
264 samples is highly consistent. Figure 4B presents a normalization of the four representative
265 curves shown in Figure 4A. The curves were normalized by subtracting the initial potential
266 value for each curve. In doing so, all curves practically collapse into an invariant shape.

267 The black line in Figure 4B depicts the average of the four curves corresponding to
268 independently run negative samples. This profile, characteristic of negative samples, is
269 distinguishable from that inherent to the specific amplification observed in samples that do
270 contain SARS-CoV-2 genetic material. Figure 4C shows the trajectories of the electric

potential associated with positive samples containing different quantities of SARS-CoV-2 synthetic genetic material (color curves).

**Figure 4**

The average progression of the electric potential in negative samples (from Figure 4B) is indicated by the gray line. The potential exhibits a distinctive, practically immediate, and sharp increase at the incubation conditions that are associated with a high initial rate of amplification. The initial slope of the potential curve is steeper in positive samples than in negative samples. However, a high sampling rate is required in the monitoring device for a clear identification of this steep initial slope. In our experiments, we achieved the resolution needed to identify the sharp slope associated with samples that contained SARS-CoV-2 genetic material by sampling at least once per second (the Arduino code is available in supplementary material; File S1). Lower sampling rates (e.g., 0.2 Hz) do not serve the purpose of clearly resolving the initial slope of the reaction in positive samples (supplementary material; Figure S3). We also observed that the evolution of each curve is consistent with the copy load in the positive samples, so that higher copy numbers originate curves with a higher initial slope than is observed for curves associated with lower loads. Since the initial rate of amplification is remarkably high in positive samples ( $> 25$ to 75 mV $s^{-1}$), the differences between slopes can be clearly established only if high sampling rates ($\sim 1$ sample $s^{-1}$: 1 Hz) are imposed.

In general, discrimination in positive samples between negative samples and positive samples with medium to high viral loads (i.e., at least 100 copies) by comparison of the potential trajectories. However, samples containing a low copy number (i.e., less than 10 gene copies) cannot be distinguished from negative samples by only comparing trajectories

(Figure 4C). The inset in Figure 4C zooms in on the first five minutes of the amplification reaction and shows that the behavior of the trajectory of the amplification reaction in positive and negative samples can be better discriminated at this first stage of the amplification. For instance, the value of the area under the curve or of $\Delta P$ versus t is distinguishably higher in positive samples than in negative samples during the first stage of the amplification. Here, we define IP3, the integral of the potential with respect to time for the first 3 minutes of reaction, as an indicator of specific amplification of genetic material in the LAMP reactions (equation 1).

$$IP_3 = \int \mathbf{\Delta P}^* \, dt \Big|_{3min} \qquad \text{equation (1)}$$

$$\mathbf{\Delta P}^* = (\Delta P_i - \Delta P_o) \qquad \text{equation (2)}$$

Here, $\Delta P_i$ is the value of electric potential measured at every sampling point and $\Delta P_o$ is the value of electric potential at the beginning of the experiment. Therefore $\mathbf{\Delta P}^*$ is the increment in potential measured at each sampling event (i.e., in our case, every second) with respect to the initial value of electric potential in the reaction mix at the initial point of the amplification. Equation 3 provides a step by step approximation of $IP_3$.

$$IP_3 \sim \Sigma_{i \text{ to } n} (\mathbf{\Delta P}^*)_i \, (\mathbf{\Delta t}) \qquad \text{equation (3)}$$

Here, n is the number of sampling points within the time frame from 0 to 3 minutes. Indeed, we found that $IP_3$ is a reliable and robust predictor that enables the consistent and rapid identification of samples containing (or not containing) SARS-CoV-2 genetic material. Figure 4C shows the evolution of the integral of $IP_3$ for the first 3 minutes of a set of LAMP reactions. Progressions corresponding to samples added with different quantities of synthetic genetic material (i.e., 10, 100, 1000, and 10000 copies of the N gene of SARS-

316 CoV-2) were compared versus three independent repeats of negative samples (i.e., samples
317 without SARS-CoV-2 genetic material). Negative samples (plotted in yellow) exhibit
318 integrals significantly lower than those calculated from the analysis of positive samples. In
319 addition, a linear correlation can be established between the logarithm of the copy number
320 and the value of the integral (Figure 4D; inset). These results suggest that $IP_3$ is a reliable
321 and quantitative indicator of the specific amplification of genetic material in simple
322 samples.

323 **qLAMP in saliva samples**

324 We then extended the use of this embodiment of qLAMP to the identification of SARS-
325 CoV-2 genetic material in saliva samples. As already mentioned, colorimetric LAMP using
326 phenol red has recently received attention as a cost-effective diagnostic method that enables
327 discrimination between COVID(+) and COVID(-) samples by naked eye inspection and is
328 therefore independent of the use of costly PCR instruments[11,33].

329 However, colorimetric LAMP exhibits its own important limitations, and its direct
330 implementation in saliva samples is technically challenging. Human saliva exhibits a wide
331 range of pH values[34,35]; therefore, even small volumes of saliva may significantly affect
332 the initial pH of the reaction mix in LAMP-based methods. Acidic saliva samples may
333 induce a premature shift in the pH (and the color) that is not associated with amplification
334 and will eventually lead to a false positive diagnosis. The direct and real-time reading of
335 electric potential throughout the amplification offers a solution to some of the limitations of
336 final-point colorimetric LAMp methods in the context of the analysis of saliva samples.

337 Figure 5A shows the results of the progression of LAMP amplification in saliva samples
338 with or without added synthetic genetic material in different quantities (i.e., in the range of

10 to 10,000 copies of the N gene of SARS-CoV-2). In this experimental set, the reaction mix contained 3–4 µL of real undiluted saliva (volume defined based in ref [15] ) from SARS-CoV-2 negative volunteers (as determined by end-point colorimetric LAMP). As before, the amplification curves that corresponded to samples spiked with SARS-CoV-2 genetic material exhibited a steep slope that was immediately observable upon initiation of the incubation. The typical smoother progression associated with negative samples (Figure 4B) was also observed in negative saliva samples. In Figure 5B, we have plotted the results from a set of experiments in which the $IP_3$ values for saliva samples with or without SARS-CoV-2 genetic material were calculated. The $IP_3$ values were clearly higher in positive samples than in negative samples. The positive samples with low to medium SARS-CoV-2 gene copy loads were also clearly distinguishable from negative samples.

**Figure 5**

The $IP_3$ value is an indicator of the extent of specific amplification that is somehow analogous to the progression of the change of color (from red-magenta to crisp yellow; Figure 5C) during the amplification in colorimetric LAMP. Indeed, the use of a commercial color sensor allows the quantitative analysis of the process of the color change during colorimetric LAMP[36] mediated by phenol red, as we and others have shown previously [11,37] (supplementary material; Figure S4). For comparison, we monitored online the change in color associated with the process of amplification in samples that contained different quantities of SARS-CoV-2 genetic material (Figure 5D).

Note that the shape of the curves that describes the change in color and the change in potential are similar. This is expected. Both processes (i.e., the change in electric potential in the reaction mix and the development of color) are cumulative processes directly related

to the release of protons during amplification. However, the time scale at which color and electric potential evolve differs quite drastically. Changes in color are observable at a much slower rate—positive and negative samples can be discriminated due to their color evolution within the first 30 minutes of reaction (supplementary material; Figure S4 A and C). Remarkably, the evolution of the $IP_3$ indicator introduced here enables a reliable discrimination between positive and negative samples within the initial 3 minutes of the reaction.

**Potential relevance and limitations**

The result presented here may be highly relevant in practical terms. The typical concentration of gene copies of SARS-CoV-2 in the saliva of positive subjects (even asymptomatic ones) is generally higher than $10^5$ $mL^{-1}$ ($10^3$ $\mu L^{-1}$). In the analysis presented here, 3–4 $\mu L^{-1}$ of undiluted saliva can be added without observing inhibitory effects in terms of the extent of the amplification. Therefore, copy number values greater than $10^3$ per assay can be expected. Based on our experiments, the limit of detection/discrimination of this method, assisted by online monitoring of the electric potential of the solution during amplification, is two orders of magnitude below this (i.e., 10–100 SARS-CoV-2 copies per assay). This suggests that this method could render reliable diagnostic results for diagnosis of COVID-19 in unextracted (undiluted or diluted) saliva samples that have even moderate or low viral loads. This hypothesis remains to be tested by the diagnostic evaluation of saliva samples from actual patients and at this point should be taken as an inference.

Several limitations of the methodology presented here should also be noted. The successful performance of this diagnostic strategy is centered on the ability to sample the electric potential (or pH) of the reaction mix frequently (the authors recommend at least at 1.0 Hz)

during the initial stage of the amplification reaction (i.e., at least during the initial three minutes). Therefore, this requires an electrode with a sufficiently fast response and a sensor capable of operating at a sufficiently high sampling rate (at least one pH measurement per second). In addition, equilibration of the electrode at the typical initial pH (or potential) of the LAMP reaction mix is desirable. Failure to do this may hinder the resolution of the readings during the first seconds of the amplification due to a lag in the response or the adjustment of the sensor to the pH conditions (supplementary material; Figure S3).

In the current developmental state of our diagnostic device, we depend on the use of commercial pH microelectrodes that are relatively expensive. For instance, we estimate that the cost of development a diagnostic unit capable of running 8 reactions simultaneously in our lab would be on the order of 10,000 USD. In addition, the use of glass or membrane-based pH microelectrodes may be a source of contamination of samples with residual DNA (from a previous positive amplification). Protocols should be established that can effectively remove residual nucleic acids after the completion of an amplification experiment from the electrode. The development of disposable and low-cost pH microelectrodes should be a priority for enabling the cost-effective use of this strategy to intensify the ability to perform label-free and portable/mobile molecular diagnostics of SARS-CoV-2 and other pathogens.

## Conclusions and outlook

Preparedness to face infectious diseases is the key to buffering the spread of epidemics and minimizing the number of human deaths. Extraction-free and portable diagnostics from saliva will greatly enable the intensification of testing efforts in the context of pandemic COVID-19 and other infectious diseases.

Here, we have introduced a strategy for reliable and consistent identification of samples containing SARS-CoV-2 genetic material. This strategy relies on the real-time monitoring of the LAMP reaction in the weakly buffered reaction mix commonly used for colorimetric LAMP. The continuous release of protons associated with the incorporation of bases into the nascent chains of DNA during amplification is measured online with a pH microelectrode that is immersed in the reaction mix incubated at 62.5 °C. We also showed that proper isothermal control and online determination of changes in potential (or pH) in the LAMP reaction mix can be appropriately accomplished using a simple Arduino-based device.

In addition, we demonstrate that the area under the curve that describes the time evolution of the values of the electric potential of the reaction mix during the first three minutes of the amplification (i.e., defined here as $IP_3$) is a reliable predictor of the extent of specific amplification occurring during the LAMP reactions. The evaluation of $IP_3$ enables the consistent discrimination between samples containing or not containing SARS-CoV-2 genetic material. We also demonstrated the feasibility of using this portable, fast, and reliable diagnostic strategy with saliva samples containing different loads of SARS-CoV-2 genetic material.

Recent reports have shown that the performance of LAMP is greatly influenced by the reaction conditions and the reagents used (i.e., primers sets, retro-transcriptases or proteases, additives, and fluorescent dyes, among others) [17,38]. The label-free qLAMP platform presented here may be highly useful in the selection of reaction reagents (i.e., alternative polymerases, additives to enhance the amplification, or primer sets) or optimization of LAMP conditions (i.e., temperatures and concentrations). The mere

comparison of the curves of evolution of protons with time under different reaction conditions provides a direct way to evaluate the effect of any modifications in the protocol on the overall performance of the amplification.

The release of protons during amplification, which is the underlying process that we are monitoring, is inherent in all nucleic acid amplification methods. Therefore, the methodology of real-time monitoring of the change in electric potential during amplification is fully translatable to other amplification schemes (i.e., qPCR and RPA, among others).

## Acknowledgments

EGG and SB acknowledge funding from doctoral scholarship provided by CONACyT (Consejo Nacional de Ciencia y Tecnología, México). GTdS and MMA acknowledge the institutional funding received from Tecnológico de Monterrey (Grant 002EICIS01 and Novus 2019) and CONACyT (Sistema Nacional de Investigadores; 66839 and 26048). The authors acknowledge the funding provided by the Federico Baur Endowed Chair in Nanotechnology (0020240I03). The authors gratefully acknowledge funding from Fundación-FEMSA and from an alumnus of Tecnológico de Monterrey who prefers to remain anonymous.

## CRediT author statement

**Mario Moisés Alvarez:** Conceptualization, Methodology, Investigation, Formal Analysis, Resources, Software, Data curation, Writing - original draft, Writing-Reviewing & Editing, Supervision, Project Administration, Funding acquisition; **Sergio Bravo-González**:

Methodology, Investigation, Data curation, Software; **Everardo González-González**: Methodology, Investigation, Resources; **Grissel Trujillo-de Santiago:** Conceptualization, Methodology, Resources, Writing-Reviewing & Editing, Supervision, Project Administration, Funding acquisition.

## Competing interest

The authors declare no competing interests.

476

477

478 # Figures and captions:

479

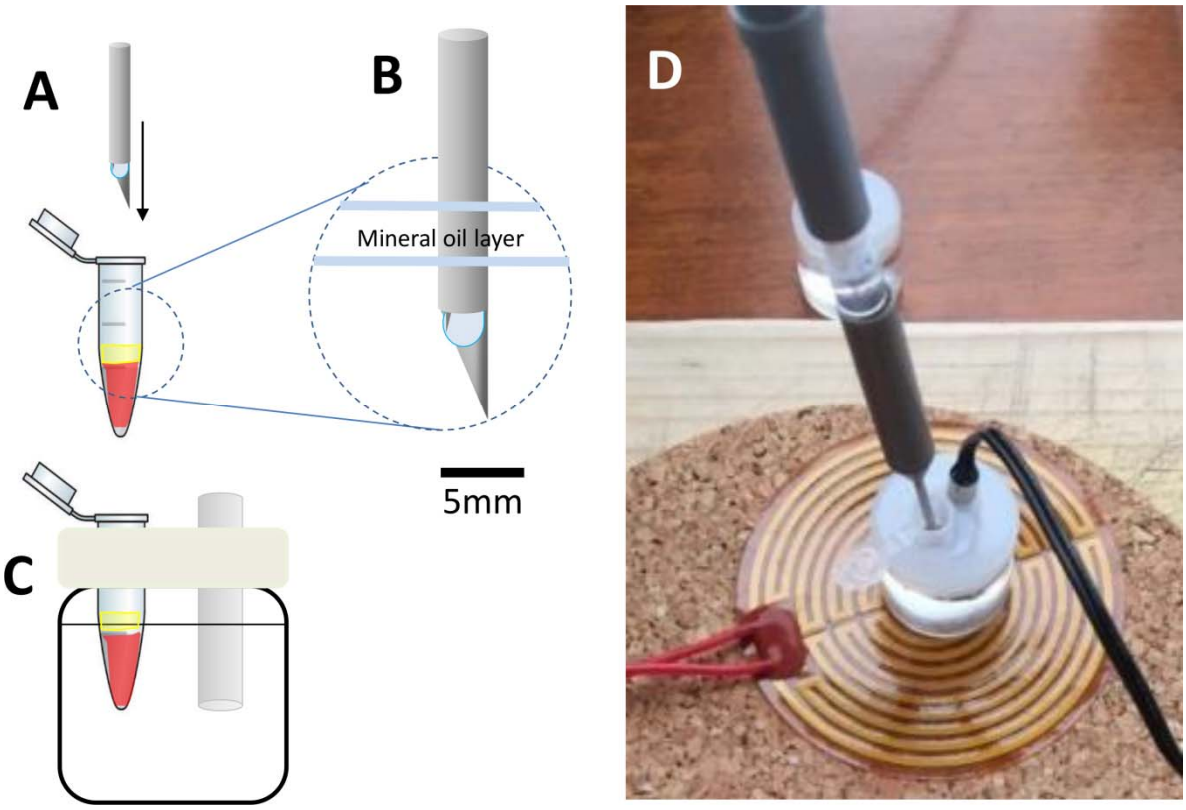


480

481 **Figure 1.** Experimental setup**.** (A) A micro pH electrode is inserted into the Loop-mediated
482 Isothermal Amplification (LAMP) colorimetric reaction mix and (B) a thin layer of oil is added
483 to avoid evaporation during incubation (C) in an oil bath. (D) Image of the actual system; a heating
484 mat connected to an Arduino-based proportional integral derivative (PID) controller is used to
485 control the temperature at 62.5 +/- 1.2 °C.
486
487
488

489

490

491

492

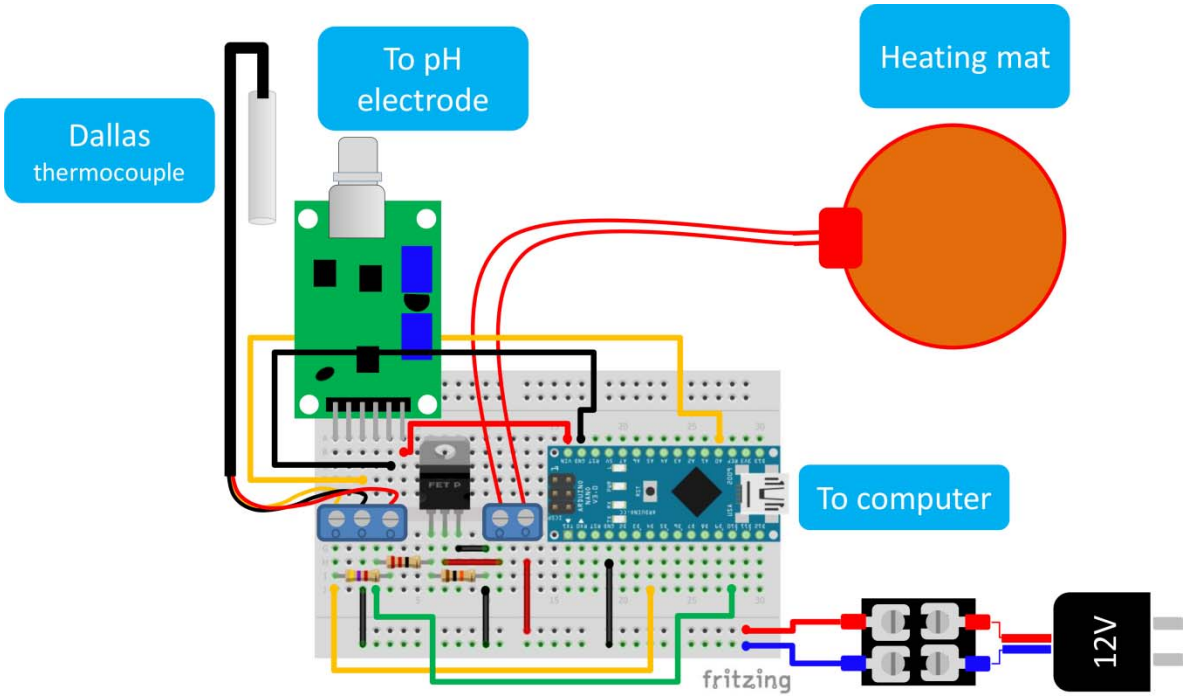


**Figure 2.** Schematic representation of the Arduino-based proportional integral derivative (PID) temperature controller and online electric potential monitoring system.

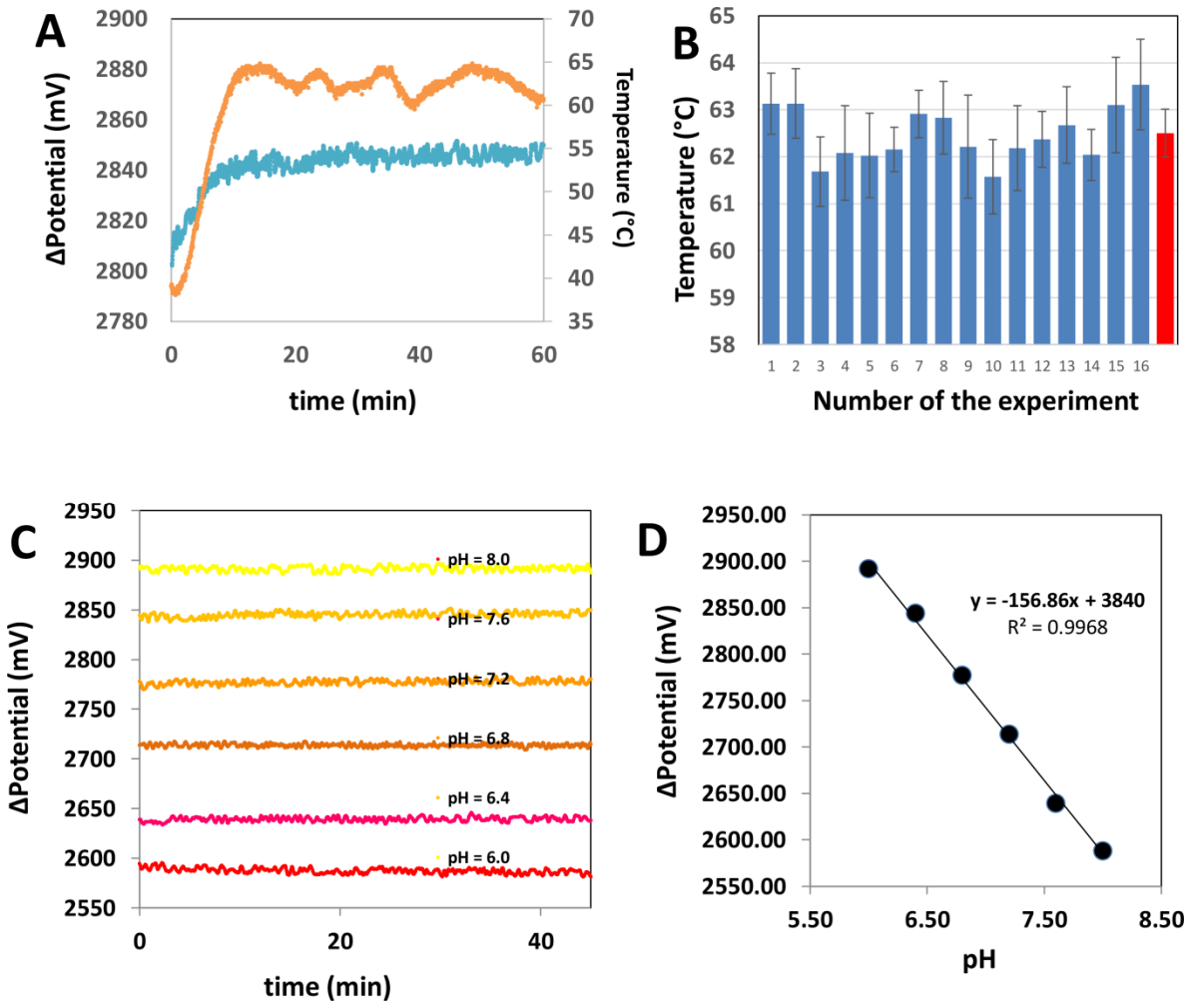


**Figure 3.** Basic characterization of the electric potential monitoring system and the Arduino-based proportional integral derivative (PID) controller. (A) The potential signal is stable at different pH values. (B) A linear dependence between pH and potential differential was observed in the entire range of pH values relevant to the Loop-mediated Isothermal Amplification (LAMP) reaction. (C) The potential differential is stable at isothermal conditions. (D) The Arduino-based PID controller is able to maintain the temperature value around the set point value (62.5 +/- 0.5° C) in a set of 16 independent experiments. The red bar indicates the average temperature and standard deviations of this set of 16 independent experiments.

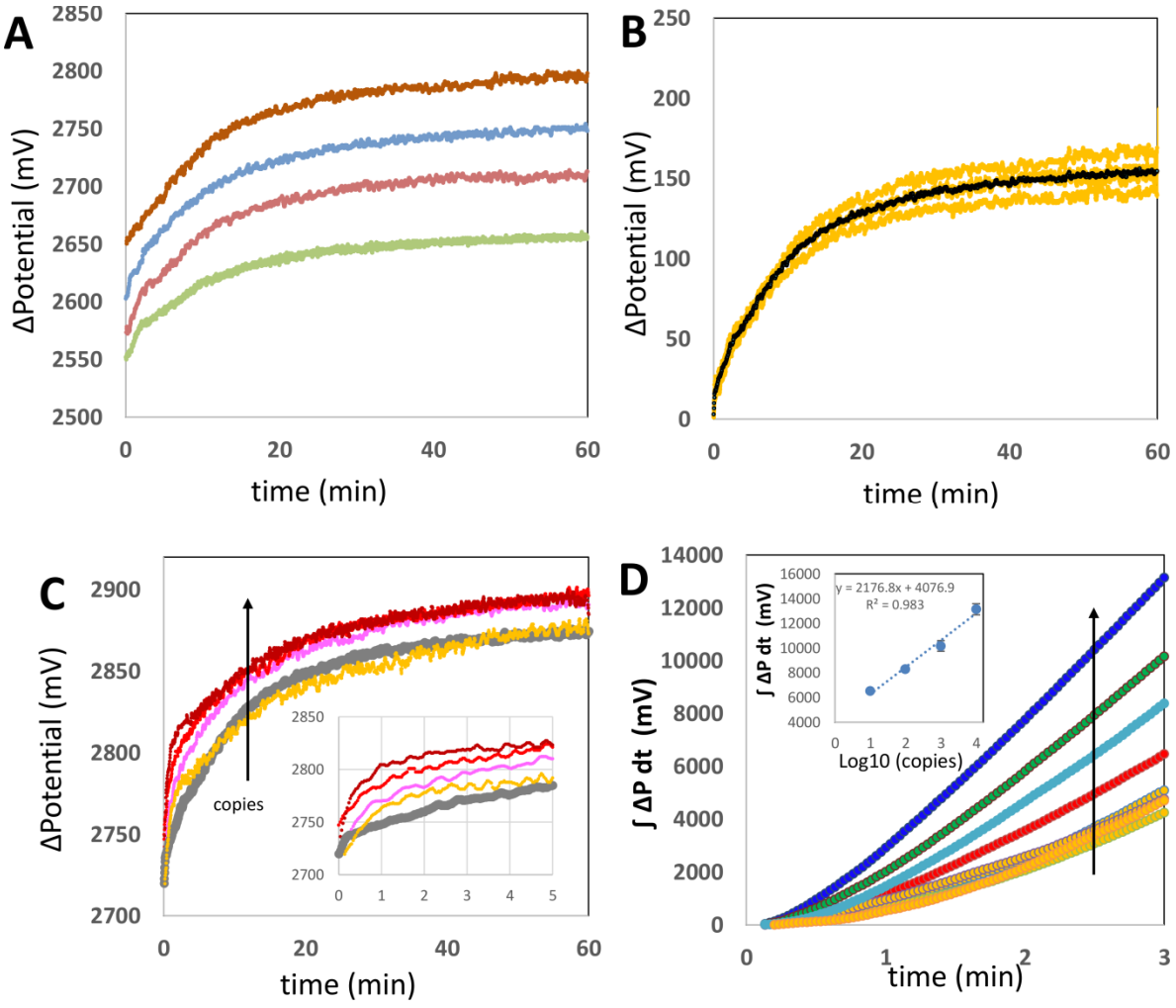


**Figure 4.** Discrimination between SARS-CoV-2 positive and negative samples using online electric potential measurements. (A) Measurement of four different negative samples (i.e., samples without SARS-CoV-2 genetic material, but containing reaction mix and primers). (B) Normalized signal of a set of four different negative samples indicated with yellow lines. Values were normalized by subtracting the initial potential value of each curve. The black line depicts the average of the four yellow trajectories and is characteristic of the progression of the Loop-mediated Isothermal Amplification (LAMP) reaction observed in negative samples. (C) Comparison of the online potential signal in samples containing 10,000 (magenta), 1000 (red), 100 (pink), and 10 (yellow) copies of synthetic SARS-CoV-2 genetic material. The average of four negative samples is depicted in gray. The inset shows a close-up of the first five minutes of the amplification reaction. (D) Plot of the integral of the differential of potential with respect to time for the first 3 minutes of amplification in samples containing different copy numbers of synthetic SARS-CoV-2 genetic material: 10,000 (dark blue), 1000 (brown), 100 (light blue), and 10 (red) copies of synthetic SARS-CoV-2 genetic material. Trends associated with negative samples are presented in blue, orange, green, and yellow.

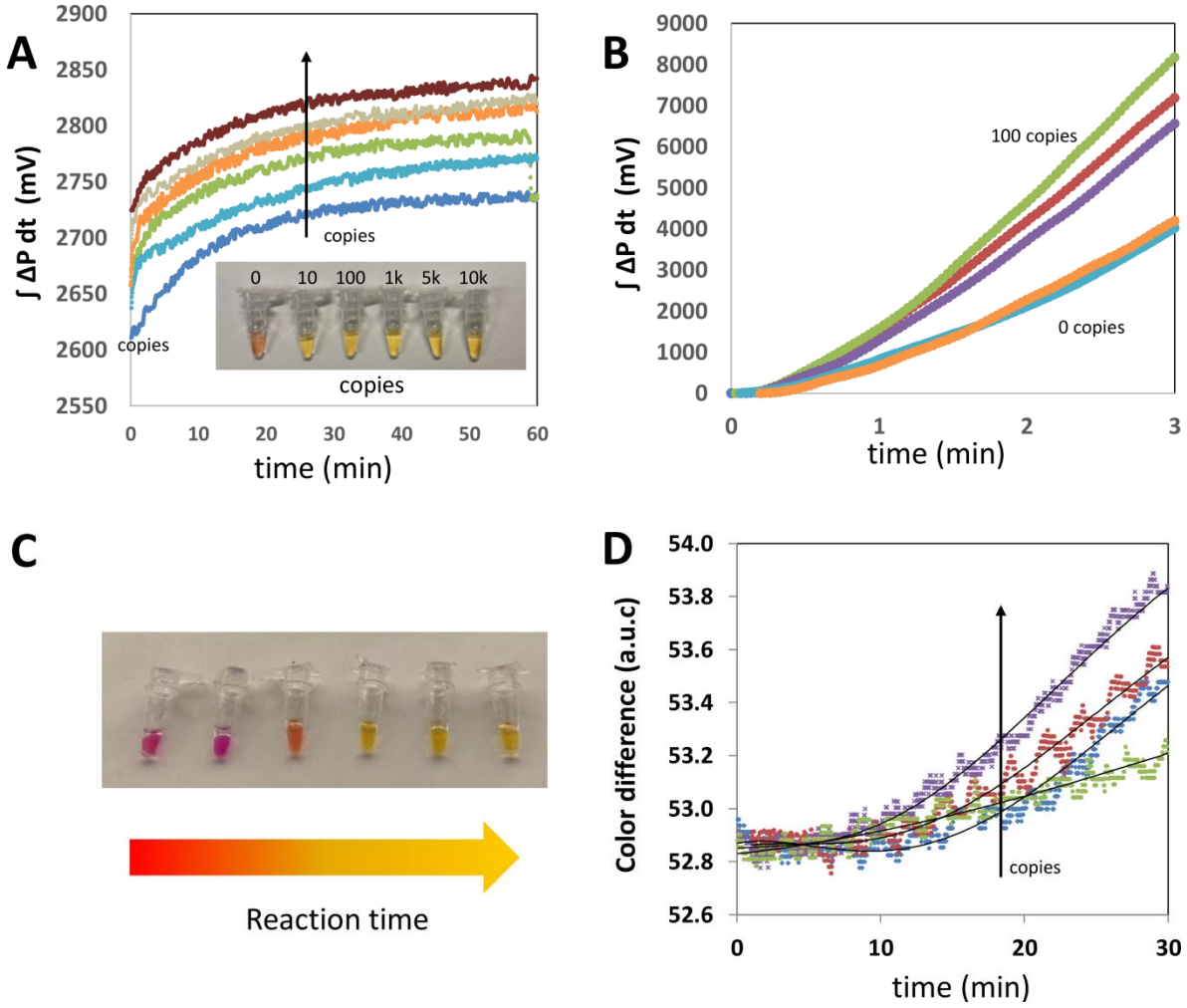


**Figure 5.** Discrimination between SARS-CoV-2 positive and negative saliva samples using online electric potential measurements. (A) Results from the online evaluation of electric potential in a saliva sample from a volunteer diagnosed as SARS-CoV-2 negative (dark blue curve) and a set of five saliva samples added with 10 (blue line), 100 (green line), 1000 (orange curve), 5000 (beige curve), and 10000 copies (brown curve) of SARS-CoV-2 genetic material. (B) Plot of the integral of the differential of potential with respect to time for the first 3 minutes of amplification in saliva samples containing different copy numbers of synthetic SARS-CoV-2 genetic material in the range of 10–100 copies (purple, green and red curves) or not containing SARS-CoV-2 genetic material (orange and blue curves). The blue curve corresponds to the analysis of an actual sample from a symptomatic patient later confirmed as SARS-CoV-2 negative by RT-qPCR. (C) Typical color progression (from red-magenta to crisp yellow in a positive sample) through colorimetric Loop-mediated Isothermal Amplification (LAMP). (D) Evolution of the difference in color (with respect to the initial red-magenta color) in positive samples containing 0 (green), 10 (blue), 100 (red), and 1000 (purple) added synthetic copies of SARS-CoV-2 genetic material.

**Table 1.** Sequences of the Loop-mediated Isothermal Amplification (LAMP) primers used for the detection of segments of genetic material encoding for the expression of the N protein of SARS-CoV-2.

| Set | Description | Primers Sequence (5'>3') |
|---|---|---|
| Primer set α | 2019-nCoV 1-F3 | *TGGACCCCAAAATCAGCG* |
| | 2019-nCoV 1-B3 | *GCCTTGTCCTCGAGGGAAT* |
| | 2019-nCoV 1-FIP | *CCACTGCGTTCTCCATTCTGGTAAATG CACCCCGCATTACG* |
| | 2019-nCoV 1-BIP | *CGCGATCAAAACAACGTCGGCCCTTG CCATGTTGAGTGAGA* |
| | 2019-nCoV 1-LF | *TGAATCTGAGGGTCCACCAA* |
| | 2019-nCoV 1-LB | *TTACCCAATAATACTGCGTCTTGGT* |

## References

[1] Home - Johns Hopkins Coronavirus Resource Center, (n.d.). https://coronavirus.jhu.edu/ (accessed September 10, 2020).

[2] M.N. Esbin, O.N. Whitney, S. Chong, A. Maurer, X. Darzacq, R. Tjian, Overcoming the bottleneck to widespread testing: A rapid review of nucleic acid testing approaches for COVID-19 detection, RNA. 26 (2020) 771–783. doi:10.1261/rna.076232.120.

[3] N. Younes, D.W. Al-Sadeq, H. AL-Jighefee, S. Younes, O. Al-Jamal, H.I. Daas, H.M. Yassine, G.K. Nasrallah, Challenges in Laboratory Diagnosis of the Novel Coronavirus SARS-CoV-2, Viruses. 12 (2020) 582. doi:10.3390/v12060582.

[4] M.P. Cheng, J. Papenburg, M. Desjardins, S. Kanjilal, C. Quach, M. Libman, S. Dittrich, C.P. Yansouni, Diagnostic Testing for Severe Acute Respiratory Syndrome-Related Coronavirus 2: A Narrative Review, Ann. Intern. Med. 172 (2020) 726–734. doi:10.7326/M20-1301.

[5] C.B.F. Vogels, A.F. Brito, A.L. Wyllie, J.R. Fauver, I.M. Ott, C.C. Kalinich, M.E. Petrone,

A. Casanovas-Massana, M. Catherine Muenker, A.J. Moore, J. Klein, P. Lu, A. Lu-Culligan, X. Jiang, D.J. Kim, E. Kudo, T. Mao, M. Moriyama, J.E. Oh, A. Park, J. Silva, E. Song, T. Takahashi, M. Taura, M. Tokuyama, A. Venkataraman, O. El Weizman, P. Wong, Y. Yang, N.R. Cheemarla, E.B. White, S. Lapidus, R. Earnest, B. Geng, P. Vijayakumar, C. Odio, J. Fournier, S. Bermejo, S. Farhadian, C.S. Dela Cruz, A. Iwasaki, A.I. Ko, M.L. Landry, E.F. Foxman, N.D. Grubaugh, Analytical sensitivity and efficiency comparisons of SARS-CoV-2 RT–qPCR primer–probe sets, Nat. Microbiol. 5 (2020) 1299–1305. doi:10.1038/s41564-020-0761-6.

[6] J.M. Sharfstein, S.J. Becker, M.M. Mello, Diagnostic Testing for the Novel Coronavirus, JAMA - J. Am. Med. Assoc. 323 (2020) 1437–1438. doi:10.1001/jama.2020.3864.

[7] A.K. Giri, D.R. Rana, Charting the challenges behind the testing of COVID-19 in developing countries: Nepal as a case study, Biosaf. Heal. 2 (2020) 53–56. doi:10.1016/j.bsheal.2020.05.002.

[8] L. Yu, S. Wu, X. Hao, X. Dong, L. Mao, V. Pelechano, W.-H. Chen, X. Yin, Rapid Detection of COVID-19 Coronavirus Using a Reverse Transcriptional Loop-Mediated Isothermal Amplification (RT-LAMP) Diagnostic Platform, Clin. Chem. 66 (2020) 975–977. doi:10.1093/clinchem/hvaa102.

[9] L.E. Lamb, S.N. Bartolone, E. Ward, M.B. Chancellor, Rapid Detection of Novel Coronavirus (COVID19) by Reverse Transcription-Loop-Mediated Isothermal Amplification, SSRN Electron. J. (2020). doi:10.2139/ssrn.3539654.

[10] Y. Zhang, N. Odiwuor, J. Xiong, L. Sun, R.O. Nyaruaba, H. Wei, N.A. Tanner, Rapid Molecular Detection of SARS-CoV-2 (COVID-19) Virus RNA Using Colorimetric LAMP, MedRxiv. 2 (2020) 2020.02.26.20028373. doi:10.1101/2020.02.26.20028373.

[11] E. González-González, I.M. Lara-Mayorga, I.P. Rodríguez-Sánchez, Y.S. Zhang, S.O. Martínez-Chapa, G.T. Santiago, M.M. Alvarez, Colorimetric loop-mediated isothermal amplification (LAMP) for cost-effective and quantitative detection of SARS-CoV-2: the change in color in LAMP-based assays quantitatively correlates with viral copy number, Anal. Methods. 13 (2021) 169–178. doi:10.1039/d0ay01658f.

[12] J. Rodriguez-Manzano, K. Malpartida-Cardenas, N. Moser, I. Pennisi, M. Cavuto, L. Miglietta, A. Moniri, R. Penn, G. Satta, P. Randell, F. Davies, F. Bolt, W. Barclay, A. Holmes, P. Georgiou, Handheld Point-of-Care System for Rapid Detection of SARS-CoV-2 Extracted RNA in under 20 min, ACS Cent. Sci. (2021). doi:10.1021/acscentsci.0c01288.

[13] X. Zhu, X. Wang, L. Han, T. Chen, L. Wang, H. Li, S. Li, L. He, X. Fu, S. Chen, M. Xing, H. Chen, Y. Wang, Multiplex reverse transcription loop-mediated isothermal amplification

combined with nanoparticle-based lateral flow biosensor for the diagnosis of COVID-19, Biosens. Bioelectron. 166 (2020) 112437. doi:10.1016/j.bios.2020.112437.

[14] N. Toppings, A. Mohon, Y. Lee, H. Kumar, D. Lee, R. Kapoor, G. Singh, L. Oberding, O. Abdullah, K. Kim, B. Berenger, D. Pillai, Saliva-Dry LAMP: A Rapid Near-Patient Detection System for SARS-CoV-2, (n.d.). doi:10.21203/rs.3.rs-141322/v1.

[15] M.A. Lalli, J.S. Langmade, X. Chen, C.C. Fronick, C.S. Sawyer, L.C. Burcea, M.N. Wilkinson, R.S. Fulton, M. Heinz, W.J. Buchser, R.D. Head, R.D. Mitra, J. Milbrandt, Rapid and Extraction-Free Detection of SARS-CoV-2 from Saliva by Colorimetric Reverse-Transcription Loop-Mediated Isothermal Amplification, Clin. Chem. 67 (2021) 415–424. doi:10.1093/clinchem/hvaa267.

[16] B.A. Rabe, C. Cepko, SARS-CoV-2 detection using isothermal amplification and a rapid, inexpensive protocol for sample inactivation and purification, Proc. Natl. Acad. Sci. U. S. A. 117 (2020) 24450–24458. doi:10.1073/pnas.2011221117.

[17] A. Alekseenko, D. Barrett, Y. Pareja-Sanchez, R.J. Howard, E. Strandback, H. Ampah-Korsah, U. Rovšnik, S. Zuniga-Veliz, A. Klenov, J. Malloo, S. Ye, X. Liu, B. Reinius, S.J. Elsässer, T. Nyman, G. Sandh, X. Yin, V. Pelechano, Direct detection of SARS-CoV-2 using non-commercial RT-LAMP reagents on heat-inactivated samples, Sci. Rep. 11 (2021) 1820. doi:10.1038/s41598-020-80352-8.

[18] N. L'Helgouach, P. Champigneux, F.S. Schneider, L. Molina, J. Espeut, M. Alali, J. Baptiste, L. Cardeur, B. Dubuc, V. Foulongne, F. Galtier, A. Makinson, G. Marin, M.C. Picot, A. Prieux-Lejeune, M. Quenot, F.C. Robles, N. Salvetat, D. Vetter, J. Reynes, F. Molina, EasyCOV: LAMP based rapid detection of SARS□CoV□2 in saliva, MedRxiv. (2020) 2020.05.30.20117291. doi:10.1101/2020.05.30.20117291.

[19] E. González-González, I.M. Lara-Mayorga, I.P. Rodríguez-Sánchez, Y.S. Zhang, S.O. Martinez-Chapa, G. Trujillo de Santiago, M.M. Alvarez, Colorimetric Loop-mediated Isothermal Amplification (LAMP) for cost-effective and quantitative detection of SARS-CoV-2: The change in color in LAMP-based assays quantitatively correlates with viral copy number., Anal. Methods. (2020). doi:10.1039/D0AY01658F.

[20] N.A. Tanner, Y. Zhang, T.C. Evans, Visual detection of isothermal nucleic acid amplification using pH-sensitive dyes, Biotechniques. 58 (2015) 59–68. doi:10.2144/000114253.

[21] M.J. Kellner, J.J. Ross, J. Schnabl, M.P.S. Dekens, R. Heinen, I. Grishkovskaya, B. Bauer, J. Stadlmann, L. Menéndez-Arias, R. Fritsche-Polanz, M. Traugott, T. Seitz, A. Zoufaly, M. Födinger, C. Wenisch, J. Zuber, A. Pauli, J. Brennecke, S. Ameres, B. Bauer, N. Beer, K.

Bergauer, W. Binder, C. Blaukopf, B. Bochev, J. Brennecke, S. Brinnich, A. Bundalo, M. Busslinger, A. Bykov, T. Clausen, L. Cochella, G. de Vries, M. Dekens, D. Drechsel, Z. Dzupinkova, M. Eckmann-Mader, U. Elling, M. Fellner, T. Fellner, L. Fin, B.V. Gapp, G. Grabmann, I. Grishkovskaya, A. Hagelkruys, B. Hajdusits, D. Haselbach, R. Heinen, L. Hill, D. Hoffmann, S. Horer, H. Isemann, R. Kalis, M. Kellner, J. Kley, T. Köcher, A. Köhler, D. Kordic, C. Krauditsch, S. Kula, R. Latham, M.C. Leitner, T. Leonard, D. Lindenhofer, R.A. Manzenreither, K. Mechtler, A. Meinhart, S. Mereiter, T. Micheler, P. Moeseneder, S. Nimpf, M. Nordborg, E. Ogris, M. Pagani, A. Pauli, J.M. Peters, P. Pjevac, C. Plaschka, M. Rath, D. Reumann, S. Rieser, M. Rocha-Hasler, A. Rodriguez, J.J. Ross, H. Scheuch, K. Schindler, C. Schmidt, H. Schmidt, J. Schnabl, S. Schüchner, T. Schwickert, A. Sommer, J. Stadlmann, A. Stark, P. Steinlein, S. Strobl, Q. Sun, W. Tang, L. Trübestein, C. Umkehrer, S. Urmosi-Incze, K. Uzunova, G. Versteeg, A. Vogt, V. Vogt, M. Wagner, M. Weissenboeck, B. Werner, R. Yelagandula, J. Zuber, A rapid, highly sensitive and open-access SARS-CoV-2 detection assay for laboratory and home testing, BioRxiv. (2020). doi:10.1101/2020.06.23.166397.

[22] J.C. Rolando, E. Jue, J.T. Barlow, R.F. Ismagilov, Real-time kinetics and high-resolution melt curves in single-molecule digital LAMP to differentiate and study specific and non-specific amplification, Nucleic Acids Res. 48 (2021) 42. doi:10.1093/NAR/GKAA099.

[23] X. Gao, B. Sun, Y. Guan, Pullulan reduces the non-specific amplification of loop-mediated isothermal amplification (LAMP), Anal. Bioanal. Chem. 411 (2019) 1211–1218. doi:10.1007/s00216-018-1552-2.

[24] E. Gonzalez-Gonzalez, G.T. Santiago, I.M. Lara-Mayorga, S.O. Martinez-Chapa, M.M. Alvarez, Portable and accurate diagnostics for COVID-19: Combined use of the miniPCR thermocycler and a well-plate reader for SARS-Co2 virus detection, MedRxiv. (2020) 2020.04.03.20052860. doi:10.1101/2020.04.03.20052860.

[25] OSF Preprints | Landscape Coronavirus Disease 2019 test (COVID-19 test) in vitro -- A comparison of PCR vs Immunoassay vs Crispr-Based test, (n.d.). https://osf.io/6eagn (accessed April 8, 2020).

[26] J.M. Rothberg, W. Hinz, T.M. Rearick, J. Schultz, W. Mileski, M. Davey, J.H. Leamon, K. Johnson, M.J. Milgrew, M. Edwards, J. Hoon, J.F. Simons, D. Marran, J.W. Myers, J.F. Davidson, A. Branting, J.R. Nobile, B.P. Puc, D. Light, T.A. Clark, M. Huber, J.T. Branciforte, I.B. Stoner, S.E. Cawley, M. Lyons, Y. Fu, N. Homer, M. Sedova, X. Miao, B. Reed, J. Sabina, E. Feierstein, M. Schorn, M. Alanjary, E. Dimalanta, D. Dressman, R. Kasinskas, T. Sokolsky, J.A. Fidanza, E. Namsaraev, K.J. McKernan, A. Williams, G.T.

714 Roth, J. Bustillo, An integrated semiconductor device enabling non-optical genome
715 sequencing, Nature. 475 (2011) 348–352. doi:10.1038/nature10242.
716 [27] D. Gosselin, M. Gougis, M. Baque, F.P. Navarro, M.N. Belgacem, D. Chaussy, A.G.
717 Bourdat, P. Mailley, J. Berthier, Screen-Printed Polyaniline-Based Electrodes for the Real-
718 Time Monitoring of Loop-Mediated Isothermal Amplification Reactions, Anal. Chem. 89
719 (2017) 10124–10128. doi:10.1021/acs.analchem.7b02394.
720 [28] D. Han, R. Chand, Y.S. Kim, Microscale loop-mediated isothermal amplification of viral
721 DNA with real-time monitoring on solution-gated graphene FET microchip, Biosens.
722 Bioelectron. 93 (2017) 220–225. doi:10.1016/j.bios.2016.08.115.
723 [29] C. Toumazou, L.M. Shepherd, S.C. Reed, G.I. Chen, A. Patel, D.M. Garner, C.J.A. Wang,
724 C.P. Ou, K. Amin-Desai, P. Athanasiou, H. Bai, I.M.Q. Brizido, B. Caldwell, D. Coomber-
725 Alford, P. Georgiou, K.S. Jordan, J.C. Joyce, M. La Mura, D. Morley, S. Sathyavruthan, S.
726 Temelso, R.E. Thomas, L. Zhang, Simultaneous DNA amplification and detection using a
727 pH-sensing semiconductor system, Nat. Methods. 10 (2013) 641–646.
728 doi:10.1038/nmeth.2520.
729 [30] S. Xie, Y. Yuan, Y. Song, Y. Zhuo, T. Li, Y. Chai, R. Yuan, Using the ubiquitous pH meter
730 combined with a loop mediated isothermal amplification method for facile and sensitive
731 detection of Nosema bombycis genomic DNA PTP1, Chem. Commun. 50 (2014) 15932–
732 15935. doi:10.1039/c4cc06449f.
733 [31] E. González-González, G. Trujillo-de Santiago, I.M. Lara-Mayorga, S.O. Martínez-Chapa,
734 M.M. Alvarez, Portable and accurate diagnostics for COVID-19: Combined use of the
735 miniPCR thermocycler and a well-plate reader for SARS-CoV-2 virus detection, PLoS One.
736 15 (2020) e0237418. doi:10.1371/journal.pone.0237418.
737 [32] Y.-P. Wong, S. Othman, Y.-L. Lau, S. Radu, H.-Y. Chee, Loop-mediated isothermal
738 amplification (LAMP): a versatile technique for detection of micro-organisms, J. Appl.
739 Microbiol. 124 (2018) 626–643. doi:10.1111/jam.13647.
740 [33] K. Nawattanapaiboon, E. Pasomsub, P. Prombun, A. Wongbunmak, A. Jenjitwanich, P.
741 Mahasupachai, P. Vetcho, C. Chayrach, N. Manatjaroenlap, C. Samphaongern, T.
742 Watthanachockchai, P. Leedorkmai, S. Manopwisedjaroen, R. Akkarawongsapat, A.
743 Thitithanyanont, M. Phanchana, W. Panbangred, S. Chauvatcharin, T. Srikhirin,
744 Colorimetric reverse transcription loop-mediated isothermal amplification (RT-LAMP) as a
745 visual diagnostic platform for the detection of the emerging coronavirus SARS-CoV-2,
746 Analyst. 146 (2021) 471–477. doi:10.1039/d0an01775b.
747 [34] M. Cohen, R. Khalaila, Saliva pH as a biomarker of exam stress and a predictor of exam

performance, J. Psychosom. Res. 77 (2014) 420–425. doi:10.1016/j.jpsychores.2014.07.003.

[35] S. Baliga, S. Muglikar, R. Kale, Salivary pH: A diagnostic biomarker, J. Indian Soc. Periodontol. 17 (2013) 461–465. doi:10.4103/0972-124X.118317.

[36] E. Gonzalez-Gonzalez, I.M. Lara-Mayorga, A. Garcia-Rubio, C.E. Garciamendez-Mijares, G.E. Guerra-Alvarez, G. Garcia-Martinez, J.A. Aguayo-Hernandez, Y.-S. Zhang, S.O. Martinez-Chapa, G. Trujillo-de Santiago, M.M. Alvarez, Scaling diagnostics in times of COVID-19: Rapid prototyping of 3D-printed water circulators for Loop-mediated Isothermal Amplification (LAMP) and detection of SARS-CoV-2 virus, Cold Spring Harbor Laboratory Press, 2020. doi:10.1101/2020.04.09.20058651.

[37] G. Papadakis, A. Pantazis, N. Fikas, S. Chatziioannidou, K. Michaelidou, V. Pogka, M. Megariti, M. Vardaki, K. Giarentis, J. Heaney, E. Nastouli, T. Karamitros, A. Mentis, S. Agelaki, E. Gizeli, Real-time colorimetric LAMP methodology for quantitative nucleic acids detection at the point-of-care, BioRxiv. (2020) 2020.07.22.215251. doi:10.1101/2020.07.22.215251.

[38] M. Janíková, J. Hodosy, P. Boor, B. Klempa, P. Celec, Loop□mediated isothermal amplification for the detection of SARS□CoV□2 in saliva, Microb. Biotechnol. 14 (2021) 307–316. doi:10.1111/1751-7915.13737.